Identification of Bax-VDAC1 complexes in digitonin-solubilized cerebellar granule neurons

Dennis B. Huckabee and **Mika B. Jekabsons**[1]
Department of Biology, University of Mississippi, University, MS 38677

Abstract

Mitochondrial outer membrane Bax oligomers are critical for cytochrome c release, but the role of resident mitochondrial proteins in this process remain unclear. Membrane-associated Bax has primarily been studied using CHAPS as the solubilizing agent, as it does not induce conformational artifacts, although recent evidence indicates it may have artifactual effects. The objective of this study was to investigate digitonin as an alternative detergent to assess Bax oligomeric state, and possible interaction with VDAC1 in cerebellar granule neurons. VDAC1 co-immunoprecipitated with Bax in digitonin extracts from healthy and apoptotic neurons. Two-dimensional blue native-SDS PAGE revealed five Bax and VDAC1 oligomers having similar masses from 120–500 kDa. The levels of two VDAC1 oligomers in Bax 1D1 immunodepleted extracts negatively correlated with levels of co-precipitated VDAC1, indicating the co-precipitated VDAC1 was derived from these oligomers. Immunodepletion with the 6A7 antibody modestly reduced the levels of Bax oligomers from apoptotic but not healthy neurons. A sixth 170 kDa oligomer containing exclusively 6A7 Bax and no VDAC1 was identified after apoptosis induction. CHAPS failed to solubilize VDAC1, and additionally yielded no distinct oligomers. We conclude that digitonin is a potentially useful detergent preserving Bax-VDAC1 interactions that may be disrupted with CHAPS.

Keywords

apoptosis; Bax; VDAC; digitonin; mitochondria; CHAPS

Introduction

Mitochondrial outer membrane permeabilization (MOMP) mediated by the multi-domain pro-apoptotic protein Bax is a critical event in the process of neuronal apoptosis (Miller *et al.* 1997). Pore formation is thought to involve a conformational change to cytoplasmic Bax that exposes a C-terminal lipid binding domain that drives its translocation to the MOM, where it inserts into the lipid bilayer to form homo-oligomeric pores (Chipuk and Green 2008; Youle and Strasser 2008; Wolter *et al.* 1997; Hsu *et al.* 1997). The upstream events waking Bax from its inactive state involves the BH3-only sub-family of pro-apoptotic proteins, but the exact process remains a topic of debate. One model proposes that selective BH3-only activator proteins (Bim, Bid), liberated from anti-apoptotic proteins by BH3-only sensitizers (e.g., Bad, Puma), transiently interact with cytosolic Bax to expose the lipid binding domain (Chipuk and Green 2008; Chipuk *et al.* 2006). An alternative model suggests that a minority of Bax exists in the lipid binding conformation in the absence of BH3-only protein activation, and is restrained from forming pores at the MOM by anti-

[1]corresponding author: 110 Shoemaker Hall, Phone: 662 915 3998, Fax: 662 915 5144, jekabson@olemiss.edu.
The authors declare no conflicts of interest.

apoptotic proteins. Activation of membrane-bound Bax by BH3-only neutralization of the anti-apoptotic proteins is thought to be the critical event, as this not only initiates oligomerization of Bax, but recruits additional Bax from the cytoplasm (Fletcher *et al.* 2008; Fletcher and Huang 2008). The latter model predicts inactive Bax hetero-oligomers at the MOM which must undergo a rearrangement to form pores. This process likely involves more than simply neutralization of anti-apoptotic proteins, as multiple Bax conformational states have been identified (Upton *et al.* 2007; Leber *et al.* 2007).

Investigations with membrane-bound Bax have been difficult due to artifacts and uncertainties resulting from detergent-induced conformational changes and/or detergent-resistant complexes (Hsu and Youle 1998; Hsu and Youle 1997). CHAPS was identified as one of the few detergents that induced neither Bax dimerization with anti-apoptotic proteins, nor an apoptotic-specific 6A7 conformation characterized by exposure of an N-terminal epitope. The latter conformational change is considered a crucial step in the process of MOMP, and can be identified with monoclonal antibody clone 6A7. However, the use of CHAPS may also be problematic, as recent studies have indicated that it can induce recombinant Bax homo-oligomerization (Brustovetsky *et al.* 2010; Bleicken *et al.* 2010) and possibly disrupt mitochondrial oligomers (Valentijn *et al.* 2008). These uncertainties, coupled with the pervasive reliance on CHAPS, may be limiting progress toward resolving further details on the mechanisms of Bax regulation and MOMP. As detailed in this study, digitonin is a useful alternative that preserves critical protein interactions not detected with CHAPS.

Resident MOM proteins that are not within the Bcl-2 family have also been implicated in MOMP by functioning as receptor, catalyst, or pore component (Polcic and Forte 2003; Shimizu *et al.* 1999; Robey and Hay 2006; Roucou *et al.* 2002). A number of reports have implicated one or more voltage-dependent anion channel (VDAC) isoforms in facilitating Bax-dependent MOMP (Pastorino *et al.* 2002; Shimizu *et al.* 1999; Majewski *et al.* 2004; Tsujimoto and Shimizu 2002; Yuan *et al.* 2008; Narita *et al.* 1998). However, others have concluded that VDAC is dispensable for MOMP (Baines *et al.* 2007; Roucou *et al.* 2002; Polcic and Forte 2003). Studies with Bak, a multi-domain pro-apoptotic protein functionally redundant with Bax, indicate an inhibitory role for VDAC. Inactive Bak is primarily mitochondrial rather than cytoplasmic, and is restrained from forming pores by interaction with VDAC2 (Cheng *et al.* 2003; Ren *et al.* 2009). Although a small amount of Bax is associated with membranes in healthy cells, there is no evidence indicating this association is by interaction with VDAC.

The majority of studies investigating Bax regulation have used hematopoetic cells or cell lines. Relatively less is known about Bax regulation in cultured neurons, an important system having relevance to neurodegenerative diseases. Cultured cerebellar granule neurons (CGNs) isolated from rat pups, a widely used model to study apoptosis, require trophic support in the form of high (25mM) extracellular K^+ and serum growth factors to suppress apoptosis (Connor *et al.* 1987; Franklin and Johnson, Jr. 1994). The collective effect of these trophic factors is elevation of cytoplasmic Ca^{2+} (by high K) and activation of plasma membrane receptor tyrosine kinases (by growth factors), both of which stimulate downstream survival kinases (e.g., Akt, Ca^{2+}-calmoldulin-dependent protein kinase II). Bax strongly associates with mitochondria and assumes the 6A7 conformation within hours of trophic factor deprivation (i.e., 3.5mM K^+, no growth factors, or low K) (Linseman *et al.* 2004), but, to our knowledge, there have been no studies investigating the role of VDAC in this process. The goal of this study was to determine the oligomeric state of Bax and its possible interaction with VDAC in trophic factor-deprived CGNs. Given recent reports of possible CHAPS interference with detection of Bax oligomers, membrane-associated Bax was studied using digitonin, an untested detergent, as solubilizing agent.

Experimental Procedures

Materials

Mouse monoclonal Bax 1D1 and 6A7 antibodies were purchased from eBioscience. Bax 6A7 antibody was also purchased from Sigma. Goat polyclonal Bax N20, goat polyclonal VDAC N18, and mouse monoclonal nuclear receptor binding protein X13 antibodies were purchased from Santa Cruz Biotechnology. Digitonin, CHAPS, BisTris, Tricine, and protease inhibitor cocktail set III were from Calbiochem. Protein G Dynabeads were from Invitrogen. Secondary horse-radish peroxidase conjugated antibodies were from Jackson ImmunoResearch. Chemiluminescent substrate and film were from Pierce. Acrylamide, PVDF membranes, milk powder, IPG strips, and Coomassie G-250 were from BioRad. Minimal essential media was from Mediatech. Characterized fetal bovine serum was from Hyclone. All other reagents of analytical grade were from Sigma.

Cerebellar granule neuron cultures

Five to seven day old Wistar rat pups (Harlan) were killed by decapitation. The cerebella were minced, trypsinized for 30min at 20°C, then triturated with flame-polished Pasteur pipettes. The suspensions were filtered through 70μm cell strainers, washed, and counted using a hemocytometer. Neurons were seeded on polyethyleneimine-coated LabTek II 2-well chambers ($4–7 \times 10^6$ per well) and maintained at 37°C/5% CO_2 in Minimum Essential Media supplemented with Earl's salts, 10% fetal bovine serum, 2 mM glutamine, 15mM glucose, and 25mM KCl. To prevent glial cell proliferation, 10μM cytosine arabinosefuranoside was added 24h after plating. Neurons between 7–10 days in culture were used for all experiments. All procedures were approved by The University of Mississippi Institutional Animal Care and Use Committee.

The experimental buffer for suppressing apoptosis (hereafter referred to as high K) contained (in mM): 116 NaCl, 25 KCl, 20 TES pH 7.35, 10 glucose, 1.3 $MgCl_2$, 1.3 $CaCl_2$, 1.2 Na_2SO_4, 0.4 KH_2PO_4, 0.2 $NaHCO_3$, 10% v/v heat-inactivated, 10kDa dialyzed fetal bovine serum. Apoptosis induction was by trophic factor deprivation using a modified buffer (hereafter referred to as low K) differing from high K in the following (in mM): 137.5 NaCl, 3.5 KCl, and 0.3% w/v fatty acid-free bovine serum albumin in place of FBS.

Imaging

Cells were incubated 5h in high or low K buffer then stained 5min with 150nM SYTO13. Images were acquired with a Zeiss Axiovert 200M epifluorescent microscope using an eGFP filter set.

Immunoprecipitation

Cells were washed once with ice-cold PBS then solubilized 30min, 4°C with shaking in 350μl lysis buffer containing 50mM NaCl, 20mM BisTris pH 7.0, 5mM aminocaproic acid, 1mM EDTA, 10% glycerol, 1% protease inhibitor cocktail, and 1% detergent (digitonin or CHAPS). In a few cases, detergent-free extracts were prepared by subjecting cells to 22 passes with a Dounce homogenizer. The extracts were centrifuged at 18–21,000 ×g, for 10min, 4°C. The supernatants were incubated overnight at 4°C on a nutator with 0.5–1.5 μg mouse monoclonal 1D1 or 6A7 antibody. Control extracts were treated with an equivalent amount of mouse monoclonal X13 antibody directly against human nuclear receptor binding protein. The antibody complexes were captured by incubation with 30–80 μl Protein G Dynabeads for 2h at 4°C, and 15min at 20°C, then washed 2–4 times in lysis buffer with 0.1–0.2 % detergent, and eluted with SDS loading buffer (60mM Tris pH 6.8, 2% SDS, 5% mercaptoethanol, 20% glycerol, 0.05% bromophenol blue) at 60°C for 10min. The samples

were separated on 4% stacking, 5–20% acrylamide resolving gels then transferred overnight at 35V, 4°C to PVDF membranes in 25 mM Tris, 192 mM glycine, 20% methanol.

Two-dimensional blue native-SDS PAGE (BN-SDS PAGE)

Cell extracts were prepared as described for the immunoprecipitations. Two-dimensional PAGE was conducted essentially as previously described (Schagger and Von 1991; Schagger *et al.* 1994). The extracts were concentrated 30–40 min at 4°C with Microcon-10 centrifugal filters (Millipore). Total protein was determined by the BCA protein assay (Pierce). Aliquots (25–40 μg protein) were supplemented with Coomassie G-250 dye at a 1:7 dye:detergent ratio, then separated on 3.5% stacking, 4–18 % resolving gels containing 50mM BisTris, 500mM aminocaproic acid pH 7.0 at 4°C. Running conditions consisted of 100V for approximately 45min, then 300V for 90–200min. The anode buffer contained 50mM BisTris pH 7.0, and the cathode buffer 15mM BisTris, 50mM Tricine, 0.02% w/v Coomassie G-250, pH 7.0. Gel filtration standards (thyroglobulin 669, apoferritin 443, β-amylase 200, alcohol dehydrogenase 150, and albumin 66 kDa) were run to estimate the relative molecular masses of the oligomers. The gels were stored at −80°C until processed. For some experiments, the extracts were subjected to overnight immunoprecipitation prior to BN-PAGE, as indicated in the figures. For second dimension SDS-PAGE, gel strips were placed in 5–8 ml SDS loading buffer, heated in boiling water for 15min, cooled to 20°C, then separated on 4% stacking, 5–20% SDS resolving gels. The samples were transferred overnight at 4°C to PVDF membranes.

Two-dimensional isoelectric focusing-SDS PAGE (IEF-SDS PAGE)

Digitonin extracts were immunoprecipitated with the 1D1 antibody as described above, except that the Dynabeads were eluted with 125μl BioRad sample buffer containing DTT (cat #163-2106). The eluates were focused on pH 3–6 IPG strips. The strips were treated 20min with 135mM iodoacetamide in BioRad equilibration buffer II (cat # 163-2108) then subjected to second dimension SDS-PAGE and blotted to PVDF membranes.

Western blot detection

Bax and VDAC were routinely detected on PVDF membranes using the SNAP ID vacuum filtration system (Millipore). Blots were blocked with 0.05% milk powder in Tris-buffered saline with 0.1% Tween-20 (TBST). Antibodies were diluted in 4 ml TBST to 0.5 – 3 μg/ml and incubated 20min. Secondary horse-radish peroxidase conjugated antibodies were diluted in TBST to 26 ng/ml and incubated 10min. The blots were visualized by incubation with chemiluminescent substrate followed by exposure to film. Prior to probing with a different primary antibody, blots were stripped in 100mM glycine, 0.1% Tween, pH 2.2 for 20–30 min.

Statistics

Two-way analysis of variance (ANOVA) and correlation analysis were performed using GraphPad Prism software. The level of significance was taken as $P<0.05$.

Results

VDAC co-immunoprecipitates with Bax

Digitonin extracts prepared from CGNs subjected to 5h high (healthy) or low (apoptotic) K were immunoprecipitated with anti-Bax 1D1 antibody then analyzed for Bax and VDAC following SDS-PAGE and Western blotting. VDAC co-immunoprecipitated with Bax in both healthy and apoptotic neurons (Fig. 1A), although the amount recovered was variable (compare Figs 1A–C) (or non-existent in two of seven experiments), and much lower than

Bax (Table 1). In this, and subsequent experiments, VDAC was detected with the N18 antibody, which according to the manufacturer (Santa Cruz Biotechnology) is recommended for detection of VDAC1, and to a lesser extent VDACs 2 and 3.. Thus, in this and subsequent experiments VDAC1 was assumed to be the predominant isoform detected. As such, VDAC detected on all blots has been designated VDAC1, but without excluding possible minor contributions from VDAC2 and/or VDAC3. Several complimentary experiments were conducted to co-immunoprecipitate Bax with VDAC1. Three polyclonal antibodies directed against different VDAC1 epitopes were employed; unfortunately, this approach was unsuccessful, as VDAC1 did not immunoprecipitate under these conditions (data not shown).

VDAC1 and Bax oligomers display similar patterns by BN-SDS PAGE

Bax interaction with VDAC1 was further tested by subjecting digitonin extracts to BN SDS-PAGE (Schagger and Von 1991; Schagger *et al.* 1994). In healthy neurons, the majority of Bax migrated in a relatively low molecular mass form that was considered predominantly monomeric based on the similar migration of SDS treated samples (Fig. 2A, B), although higher-order oligomers (e.g., dimers, trimers) may be present given the broader staining pattern. As Bax is predominantly cytoplasmic in healthy cells, most, if not all, of this low molecular mass population is likely to be derived from the cytoplasm. A minority of Bax migrated as five distinct oligomers having relative masses >100kDa (Fig. 2A). Most of the oligomers were identified in every preparation, with the exception being oligomer 2 (detected in 3 of 5 preparations). When the blots were re-probed for VDAC1, a similar five-oligomer pattern was observed, raising the possibility that VDAC1 forms multiple complexes with Bax in healthy CGNs. It is worth noting that VDAC1 was more easily detected on the blots (typically 0.5–1 min vs. 3–8 min film exposures for VDAC1 and Bax, respectively), which is consistent with a higher abundance of VDAC1 to Bax. The pattern persisted in neurons subjected to low K, (Fig. 3A), with Bax oligomer 2 again inconsistently detected (identified in 4 of 5 preparations). However, an additional Bax complex migrating between oligomers 1 and 2 (and designated as oligomer 1A, Fig. 3A) was identified in all five apoptotic extracts. The 1A oligomer did not consistently coincide with a VDAC1 oligomer, suggesting it may not interact with VDAC1. Appearance of oligomer 1A coincided with immunoprecipitation of active 6A7 Bax (Fig. 3B), a 4.2±2.8-fold (mean±SD, n=2) greater recovery of cytochrome c in crude cytoplasmic fractions (Fig. 3C), and nuclear DNA condensation/fragmentation and cell shrinkage (Fig. 3D), indicative of apoptosis (Fig. 3E).

The relative molecular masses were calculated from the migration rates of gel filtration standards run in parallel to determine if the oligomer patterns could represent Bax-VDAC1 complexes (Table 2). Analysis of each oligomer set by 2-way ANOVA (with protein type [Bax/VDAC] and treatment [high/low K] as main effects) indicated neither a significant effect of protein type, consistent with each numbered Bax/VDAC1 oligomer existing as a single complex, nor of treatment, suggesting no gross rearrangements during apoptosis.

No detectable loss of VDAC1 oligomers following Bax immunodepletion, but residual levels of two VDAC1 oligomers negatively correlate with co-precipitated VDAC1

To determine if the overlapping oligomers reflect interactions or coincidental co-migration of separate complexes, the extracts were immunodepleted of Bax with the 1D1 antibody, and then processed by BN SDS-PAGE (Fig. 4). The oligomers were stable with overnight control immunodepletions, although Bax oligomer 2 levels were generally lower than in extracts not subjected to this procedure. Bax 1D1 immunoprecipitation successfully depleted the extracts of oligomers 1, 2, 4, and 5 (Fig. 4A, B, D, E), yet the abundance (Table 3) and molecular mass (data not shown) of the corresponding VDAC1 oligomers did not

significantly differ from controls, potentially indicating that the similar patterns reflect coincidental co-migration. The 1D1 antibody is generally considered to bind Bax independent of its conformation, yet it was ineffective in immunoprecipitating oligomer 3 (based on the fact that its molecular mass did not significantly differ from the corresponding controls; data not shown).

The considerable variation in VDAC1 recovered by co-immunoprecipitation (Fig. 1) could be a factor contributing to no change in VDAC1 oligomer levels following 1D1 immunodepletion. If co-immunoprecipitated VDAC1 is derived from one or more of the oligomers, then a negative correlation should exist with the residual VDAC1 oligomer in the immunodepleted extracts. Consequently, the 1D1-depleted VDAC1 oligomer intensities were plotted against co-precipitated VDAC1 levels (Fig. 5). Significant negative correlations were found for oligomers 1 and 5 (Fig. 5A, E), consistent with immunoprecipitated VDAC1 coming from these BN oligomers, but not from oligomers 2 or 4. No significant correlations occurred, as expected, when the VDAC1 oligomer intensities from the control depletions were plotted against VDAC1 recovered from the 1D1 precipitates (data not shown).

Complete loss of Bax oligomer 1A and partial loss of oligomers 1, 3, 4, and 5 following immunodepletion of 6A7 Bax

To further test if Bax oligomer 1A interacts with VDAC1, and to additionally determine if any other oligomers contain the active, 6A7 conformation, extracts were immunoprecipitated with the Bax 6A7 antibody, then subjected to BN SDS-PAGE. Immunodepletion did not reduce the abundance of the Bax oligomers in healthy neurons (Fig. 6A, C), but completely depleted the apoptotic extracts of the 1A oligomer (Fig. 6B; the 6A7 depleted 1A signals were 10 ± 3 % of controls). Additionally, Bax oligomers 1, 3, 4, and 5 levels in apoptotic extracts tended to be lower than those from healthy neurons (Fig. 6C). Two-way ANOVA indicated a borderline significant (P=0.049) main effect of low K on Bax oligomer levels, although post-hoc tests revealed that none of the low K means differed significantly from the corresponding high K means. There was no significant main effect of oligomer (P=0.489), indicating that the effect of 6A7 depletion did not differ between the Bax oligomers. Two-way ANOVA of residual VDAC1 oligomers indicated no significant main effect of low K (P=0.133), or oligomer (P=0.712) (data not shown). Analysis of the 6A7 immunoprecipitates confirmed the presence of Bax in the low K extracts, although some was also detected in high K (Fig. 6D). VDAC1 was not detected as a co-precipitate in the 6A7 samples, while it was in parallel 1D1 positive controls (Fig. 6D). It is noteworthy that the recovery of some 6A7 Bax from high K extracts was not associated with Bax oligomer depletion (Fig. 6C), suggesting the 'monomeric' pool as the source.

An acidic shift in the isoelectric point of Bax coincides with appearance of 6A7 oligomer 1A

To determine if formation of Bax oligomer 1A is associated with a post-translational modification, 1D1 immunoprecipitates were subjected to two-dimensional isoelectric focusing (IEF) SDS-PAGE and western blotting (Fig. 7A). In high K, a broad Bax band was detected close to the predicted 5.1 isoelectric point of unmodified Bax; surprisingly, three alternate forms were also observed, at approximately pH 3.3, 4.6, and 5.8. In low K, the native pH 5.1 band largely disappeared, while a new one appeared at approximately pH 4.0, consistent with a phosphorylation event. Immunodepletion with the 6A7 antibody prior to 1D1 immunoprecipitation and IEF SDS-PAGE resulted in substantial reduction in the level of the pH 4 Bax (Fig. 7B), consistent with the involvement of this post-translational modification in the 6A7 conformational change.

Discrete Bax oligomers are not observed with CHAPS, which does not extract VDAC1

Select non-ionic detergents, including Triton X-100 and NP-40, have been shown to induce the 6A7 conformation to varying degrees, whereas the zwitterionic detergent CHAPS does not. The fact that 6A7 Bax was recovered in digitonin extracts prepared from healthy neurons (Fig. 6D), coupled with no previously published reports with digitonin, prompted a direct comparison with CHAPS. Healthy and apoptotic CGNs prepared with CHAPS and digitonin were immunoprecipitated with the 6A7 antibody (Fig. 8A), and the healthy depleted extracts were subjected to BN SDS-PAGE. In the immunoprecipitates, densitometry indicated that recovery of 6A7 Bax in the CHAPS-solubilized high K extract was less (26% of low K) than that recovered in the digitonin high K extract (58% of low K). No VDAC1 was detected in the 6A7 immunoprecipitates, but, surprisingly, VDAC1 was also not detected in the extracts prepared with CHAPS (Fig. 8A). Because CHAPS failed to solubilize VDAC1, it was predicted that the Bax oligomers would be disrupted if their presence depended on interaction with VDAC1. Analysis of the 6A7 depleted extracts revealed that the Bax oligomers were readily detected with digitonin but not CHAPS (Fig. 8B), the latter of which resulted in an extensive smear throughout the bottom half of the BN gel, with no distinct monomer apparent.

To determine if greater recovery of 6A7 Bax with digitonin was due to a detergent-induced conformational artifact, or to solubilization of a CHAPS-resistant pool of active Bax, a cytosolic extract was prepared in detergent-free lysis buffer. The extract was aliquoted equally then supplemented with 1% digitonin or CHAPS and immunoprecipitated with the 6A7 antibody (Fig. 8C). No Bax was detected with CHAPS, whereas a small quantity (relative to total starting amount) was recovered with digitonin, indicating that the latter detergent induces the 6A7 conformation in a small percentage of Bax rather than solubilizing a CHAPS-resistant pool. It is important to note that the digitonin-induced artifact cannot explain formation of the Bax oligomers, as they are not immunodepleted with the 6A7 antibody (Fig. 6A–C).

The crude membrane fractions from the detergent-free homogenates were also solubilized with digitonin or CHAPS to determine if the inability to detect distinct oligomers with CHAPS (Fig. 8B) was due to the extended overnight incubation and immunoprecipitation procedure. The pellets were detergent solubilized for 30min, clarified by centrifugation, then immediately subjected to BN-SDS PAGE. The result was similar to the overnight incubation in that Bax was present as a smear, with no distinct higher molecular mass oligomers, and no detectable VDAC1 (data not shown).

Discussion

A principle finding of this study is that endogenous VDAC1 co-immunoprecipitates with endogenous Bax in digitonin-solubilized primary cultured neurons (Figs. 1, 4, 6). The interaction was observed about 75% of the time, and in these experiments recovered VDAC1 was very low relative to Bax. Such low recoveries could indicate stability problems of the immunocaptured complexes, or simply low incidence of *in situ* interaction. Irrespective of the low recovery, the fact that the interaction was observed in both healthy and apoptotic CGNs suggests that it is not directly involved in MOMP. This is further supported by the finding that VDAC1 does not consistently align with the apoptotic-specific 1A oligomer by BN SDS-PAGE (Figs. 3A, 4E). Shimizu et al (Shimizu *et al.* 1999) co-immunoprecipitated liposome reconstituted VDAC with recombinant Bax, but, in contrast to our results, showed that the interaction in PC12 cells was restricted to cells undergoing apoptosis. The contrasting results may be due to differences in cell type and/or solubilization conditions. Despite several failed attempts to confirm the interaction by co-immunoprecipitation of Bax with VDAC1 (likely due to the VDAC antibodies' inability to

bind digitonin-masked VDAC1 epitopes), these data suggest that membrane-associated Bax in healthy cells (Hsu *et al.* 1997; Valentijn *et al.* 2008) may at least partly result from interaction with VDAC1.

A Bax oligomer was recently identified in healthy mouse mammary epithelial cell membranes using BN-PAGE (Valentijn *et al.* 2008). Similarly, in our experiments with healthy CGNs, a small amount of Bax existed as five high molecular mass oligomers, which were additionally found to have a similar migration pattern to five VDAC1 oligomers (Figs. 2, 3, 4, 6; Table 2). The possibility that co-immunoprecipitated VDAC1 was derived from one or more of these putative complexes was not, however, supported by Bax immunodepletion experiments, which affected neither the amount (Table 3) nor the relative molecular mass of the corresponding VDAC1 oligomers. This finding suggests that the overlapping patterns represent coincidental co-migration, and that co-immunoprecipitation of VDAC1 is from an oligomer not identified by BN SDS-PAGE. However, when taking into account the variable recovery of VDAC1 in the 1D1 immunoprecipitates, it is possible that at least oligomers 1 and 5 represent Bax-VDAC1 complexes, as residual VDAC1 levels following Bax 1D1 immunoprecipitation negatively correlated with the amount of co-immunoprecipitated VDAC1 (Fig 5A, E). Further evidence supporting an interaction comes from the finding that VDAC1 solubilization appears necessary to observe the Bax oligomers (Fig. 8), although it is possible that CHAPS destabilizes coincidentally migrating Bax oligomers. Taken together, the findings that (a) Bax oligomers 1 and 5 exhibit similar molecular masses to VDAC1 oligomers 1 and 5, (b) the levels of residual VDAC1 oligomers 1 and 5 negatively correlate with co-immunoprecipitated VDAC, and (c) the absence of Bax oligomers 1 and 5 under conditions that do not solubilize VDAC1 oligomers, suggest that these oligomers represent Bax-VDAC1 complexes. Given that Bax oligomer 3 was immune to 1D1 immunodepletion while VDAC1 oligomer 4 tended to negatively correlate with co-precipitated VDAC (Fig. 5D), oligomers 3 and 4 may also reflect interaction of Bax with VDAC1.

The inability to detect VDAC1 oligomer depletion following Bax 1D1 immunoprecipitation seemingly contradicts the scheme above that Bax interacts with VDAC through at least two of the BN-PAGE oligomers. However, the low abundance of Bax relative to VDAC1 oligomer is a crucial feature that may reconcile these observations. The fact that (a) VDAC1 was present exclusively in oligomeric form, while the overwhelming majority of Bax was 'monomeric' and (b) extended film exposure was required to detect the Bax oligomers, together suggest greater amounts of VDAC1 than Bax in each respective oligomer. From this perspective, it's possible that each VDAC1 spot consists predominantly of VDAC1 oligomer lacking Bax, together with a small fraction which forms a complex with Bax. Such a scenario is consistent with the low levels of VDAC1 recovered by Bax 1D1 immunoprecipitation (while the much greater Bax recovery is attributed primarily to monomer). Given the relatively low resolving power of BN-PAGE, it is not surprising that Bax-VDAC1 complexes would be indistinguishable from the corresponding Bax-free VDAC1 oligomers, particularly if monomeric Bax interacts with a high molecular mass VDAC1 oligomer. VDAC is known to form quaternary structures, as homo-oligomers, and/or contact site complexes containing the adenine nucleotide translocase and associated proteins (e.g., cyclophilin D, creatine kinase) (Grimm and Brdiczka 2007). Heterogeneous VDAC oligomers from dimers to twenty-mers have been identified by atomic force microscopy (Goncalves *et al.* 2007; Hoogenboom *et al.* 2007). Either contact site complexes or larger homo-oligomers can readily account for the relative molecular masses of the observed VDAC oligomers. Thus, variability in the amount of co-immunoprecipitated VDAC1, coupled with depletion of only a small fraction of each VDAC1 spot has the potential to make detection of significant changes in the levels of VDAC1 oligomers difficult.

In healthy neurons, different Bax conformational states have been identified, as evidenced by the finding that the 1D1 antibody, which is generally considered to recognize Bax irrespective of its conformation, was unable to immunodeplete oligomer 3 (Fig. 4). The 1D1 epitope (amino acids 3–16) in Bax oligomer 3 is therefore masked, either by one or more domains of the protein, or by the lipid-detergent micelle. In healthy neurons, oligomer 3 also resisted immunodepletion by the 6A7 antibody (Figs. 6A, C), which binds to the epitope comprising amino acids 12–24. Therefore at least two conformational states can be distinguished in healthy neurons- 1D1/6A7 inaccessible (oligomer 3), and 1D1 accessible/ 6A7 inaccessible (monomer, oligomers 1, 2, 4, 5).

In apoptotic neurons, a third, 6A7 conformation was apparent in the apoptotic-specific 1A oligomer, and, to a lesser extent, in oligomers 1, 3, 4, and 5 (Figs. 6B, C). Based on a number of studies, Leber et al (Leber *et al.* 2007) proposed that membrane-associated Bax exists in 4 states: 6A7 inaccessible and loosely associated with the membrane surface, 6A7 inaccessible and membrane inserted, 6A7 accessible and membrane inserted, and 6A7 accessible and oligomerized. The current results are compatible with this proposal. The 1D1 accessible/6A7 inaccessible form (oligomers 1, 2, 4, 5 in high K) may represent inactive, surface-associated Bax that interacts with VDAC1, while the 1A 6A7 form is likely the membrane inserted, oligomerized, pore forming state. While the results presented here indicate that the 1A oligomer is not associated with VDAC1, a potential interaction with VDAC2 or 3 cannot be excluded given the preferential binding of the N18 antibody to VDAC 1. Intermediate between these extremes, the 1D1 and 6A7 inaccessible form (oligomer 3 in high K) may reflect the membrane inserted, but still 'inactive' form, while the 1D1 and 6A7 accessible form bound to VDAC1 (a fraction of oligomers 1, 3, 4, and 5 in low K) may represent the membrane inserted, 'primed' for 1A oligomerization form. However, it is important to emphasize that we have no evidence indicating the functional role of these oligomers in the process of MOMP.

Despite modest reductions in Bax oligomers 1, 3, 4, and 5 in low K extracts immunodepleted with the 6A7 antibody (Fig. 6C), VDAC1 was neither identified as a co-precipitate with 6A7 Bax (Fig. 6D) nor significantly depleted from the extracts (data not shown). This is not surprising given that complete depletion of Bax with the 1D1 antibody (with exception of oligomer 3) yielded no change in VDAC1. Similarly, the yield of co-precipitated VDAC1 was, on average, only 1.6–1.7 times greater than background with the 1D1 antibody, so the quantity of co-precipitated VDAC1 is expected to be closer to the limit of detection given the lower quantity of Bax oligomer precipitated with the 6A7 antibody. Additionally, it is possible that the interaction of 6A7 Bax with VDAC1 is less stable than the inactive conformation.

While the functional significance of the Bax-VDAC1 interaction remains to be determined, one hypothesis to consider is that, in healthy neurons, VDAC1 plays a role in restraining Bax from transitioning to its active conformation, and hence serves as a checkpoint preventing inappropriate MOMP. This is consistent with previous findings that (a) liposomes, but not mitochondria, induced recombinant Bax into the 6A7 conformation (Yethon *et al.* 2003), and (b) mouse embryonic fibroblasts null for VDACs 1 and 3, and acutely depleted of VDAC2 by siRNA, exhibited enhanced death mediated by the apoptosis inducer staurosporine (Baines *et al.* 2007). Furthermore, VDAC2 has been shown to restrain Bak, a protein functionally redundant with Bax (Cheng *et al.* 2003). While this is consistent with a role for VDAC1 in preventing premature Bax activation, it is possible that other, yet to be identified proteins present within these complexes, are also critical for restraining Bax. Others have proposed that restraint of Bax and Bak at the MOM is due to direct or indirect interaction with one or more anti-apoptotic proteins (e.g., Bcl-2, Bcl-xL) (Polcic and Forte 2003; Leber *et al.* 2007; Fletcher and Huang 2008). From a series of yeast overexpression

and knockout studies, Polcic and Forte (Polcic and Forte 2003) found no effect of POR1 (the yeast equivalent of VDAC) knockout on Bax-dependent toxicity or on protection by Bcl-xL, while Harris et al (Harris *et al.* 2000) showed POR1/POR2 double knockouts had increased sensitivity to Bax toxicity. Endogenous POR2 expression in the former study is a notable difference that could account for the contrasting results. Taken together, it is reasonable to propose that restraint of a small Bax population by formation of MOM oligomers with VDAC1 as well as anti-apoptotic proteins may be a contributing factor to neuronal viability. Further experiments are necessary to determine if the oligomers are functionally important in protecting against apoptosis, and harbor anti-apoptotic Bcl-2 family members.

Formation of the 6A7 conformation coincides with an acidic shift in the isoelectric point of Bax to about 4.0 (Fig. 7A). Such a shift has been reported in HepG2 cells by Kim et al (Kim *et al.* 2006), who additionally demonstrated that (a) 6A7 immunoprecipitated Bax exhibited an isoelectric point of 4.0, and (b) a Thr167Asp mutation prevented this shift, consistent with a phosphorylation event accounting for the change. Consistent with Kim et al (Kim *et al.* 2006), 6A7 immunodepletion substantially reduced the intensity of the Bax pH 4.0 form (Fig. 7B), suggesting post-translational modification is involved in triggering the 6A7 conformation. Glycogen synthase kinase 3β has been implicated in phosphorylating Bax on Ser163 in cerebellar granule neurons to promote its accumulation in mitochondria (Linseman *et al.* 2004), and could potentially account for the acidic shift observed in the current experiments. Taken together, these data implicate phosphorylation of neuronal Bax as a key event in Bax transition to the 6A7 conformation.

The advantages and disadvantages of digitonin vs. CHAPS can be highlighted by comparison of our results to a recent study using a similar approach. As mentioned earlier, Valentijn et al (Valentijn *et al.* 2008) identified a ≈200 kDa Bax oligomer by BN PAGE from healthy mouse mammary epithelial cells solubilized with CHAPS. Interestingly, this oligomer was not detected with the 5B7 antibody (which is the mouse-specific equivalent of the 1D1 antibody), and was proposed to be unstable with prolonged exposure to CHAPS, as it was not detected by gel filtration (Valentijn *et al.* 2008). In light of our results, this complex is similar to the 270–300 kDa 1D1-resistant oligomer 3 identified in digitonin-extracted neurons. In our hands, however, even limited use of CHAPS did not yield discrete Bax oligomers, suggesting that this detergent either failed to solubilize, or stabilize the oligomers. The data are consistent with the former possibility given the absence of soluble VDAC1 oligomers with CHAPS (Fig. 8A, B). It is possible that the low salt conditions used in this study (in contrast to 0.5M aminocaproic acid used in (Valentijn *et al.* 2008)) hindered CHAPS solubilization of VDAC1. It is also worth mentioning that CHAPS appeared to shift the Bax monomer to a higher molecular mass smear (Fig. 8), consistent with non-specific oligomerization, as recently observed with recombinant Bax under relatively low salt conditions (Brustovetsky *et al.* 2010; Bleicken *et al.* 2010). Since such a smear was not apparent in (Valentijn *et al.* 2008), high salt may also be important in attenuating artifactual CHAPS oligomeric effects.

Solubilization of apoptotic CGNs with both digitonin and CHAPS resulted in greater recovery of immunoprecipitated 6A7 Bax compared to healthy CGNs (Fig. 8A). At least part of the higher 6A7 yield with digitonin can be attributed to solubilization and precipitation of the 1A oligomer that was not seen in healthy neurons (Fig. 6). The fact that greater 6A7 Bax recovery also occurred with CHAPS suggests that this detergent is also effective in solubilizing the 1A oligomer, which is not associated with VDAC1. However, it's unclear if the 1A oligomer remains intact upon solubilization, as apoptotic CHAPS extracts have not been analyzed by BN SDS-PAGE. It would be difficult to determine if the 1A oligomer is stable with CHAPS (at least under the experimental conditions used in this study), as it would migrate within the non-specific oligomerized smear. Accordingly,

NIH-PA Author Manuscript

NIH-PA Author Manuscript

NIH-PA Author Manuscript

CHAPS does not solubilize Bax oligomers 1–5, possibly because VDAC1 is not extracted, whereas it appears to solubilize the VDAC1-free oligomer 1A. Taken together, these data indicate that there are limitations in the use of CHAPS to study native, membrane inserted Bax, and that digitonin, by virtue of its ability to resolve healthy and apoptotic-specific Bax oligomers, may be a useful alternative. The fact that CHAPS has been used in most Bax studies could explain why the interaction with VDAC1 has not previously been detected. A caveat with using digitonin is its mild effect on inducing the 6A7 conformation. This is unlikely to be the cause of Bax oligomer formation, as these oligomers extracted from healthy neurons were resistant to immunoprecipitation with the 6A7 antibody (Figs 6, 8). Hence, the conformational effect must be restricted to low molecular mass, monomeric, Bax, and is different from that induced by low K, as the 1A oligomer was not detected in high K. This could indicate that the pre-requisite for oligomerization is not only the 6A7 conformation, but a hydrophobic (lipid) environment.

In summary, co-immunoprecipitation experiments have identified VDAC1 as an interacting partner with Bax in both healthy and apoptotic neurons solubilized with digitonin. At least two of five co-migrating Bax and VDAC1 oligomers identified by BN-SDS PAGE may be the source of the co-immunoprecipitated VDAC1. In healthy neurons, none of the oligomers contained active, 6A7 Bax, and thus do not reflect pore-forming complexes. The five oligomers were not detected with the commonly used detergent CHAPS, which is likely due to its inability to solubilize VDAC1. A small fraction of Bax within these oligomers assumed the 6A7 conformation upon induction of apoptosis, but most active Bax was localized to a sixth, ≈170kDa oligomer that was not associated with VDAC1. This apoptotic-specific oligomer is suggested to be the only pore-forming complex responsible for MOMP. We speculate that the Bax-VDAC1 oligomers present in healthy neurons represent sites of Bax restraint, similar to VDAC2 and Bak, preventing premature assembly of the 170kDa oligomer, and thus MOMP. Further experiments are necessary to determine if anti-apoptotic proteins are present in these oligomers, and whether they are important in suppressing MOMP.

Acknowledgments

Abbreviations

MOM	mitochondrial outer membrane
MOMP	mitochondrial outer membrane permeabilization
CGN	cerebellar granule neuron
BN SDS-PAGE	two dimensional blue native, sodium dodecylsulphate-polyacrylamide gel electrophoresis
CHAPS	3-[(3-Cholamidopropyl)dimethylammonio]-1-propanesulfonate
IPG	immobilized pH gradient

Reference List

Baines CP, Kaiser RA, Sheiko T, Craigen WJ, Molkentin JD. Voltage-dependent anion channels are dispensable for mitochondrial-dependent cell death. Nat Cell Biol. 2007; 9:550–555. [PubMed: 17417626]

Bleicken S, Classen M, Padmavathi PV, Ishikawa T, Zeth K, Steinhoff HJ, Bordignon E. Molecular details of Bax activation, oligomerization, and membrane insertion. J Biol Chem. 2010; 285:6636–6647. [PubMed: 20008353]

Brustovetsky T, Li T, Yang Y, Zhang JT, Antonsson B, Brustovetsky N. BAX insertion, oligomerization, and outer membrane permeabilization in brain mitochondria: Role of permeability transition and SH-redox regulation. Biochim Biophys Acta. 2010; 1797:1795–1806. [PubMed: 20655869]

Cheng EH, Sheiko TV, Fisher JK, Craigen WJ, Korsmeyer SJ. VDAC2 inhibits BAK activation and mitochondrial apoptosis. Science. 2003; 301:513–517. [PubMed: 12881569]

Chipuk JE, Bouchier-Hayes L, Green DR. Mitochondrial outer membrane permeabilization during apoptosis: the innocent bystander scenario. Cell Death Differ. 2006; 13:1396–1402. [PubMed: 16710362]

Chipuk JE, Green DR. How do BCL-2 proteins induce mitochondrial outer membrane permeabilization? Trends Cell Biol. 2008; 18:157–164. [PubMed: 18314333]

Connor JA, Tseng HY, Hockberger PE. Depolarization-and transmitter-induced changes in intracellular Ca2+ of rat cerebellar granule cells in explant cultures. J Neurosci. 1987; 7:1384–1400. [PubMed: 2883269]

Fletcher JI, Huang DC. Controlling the cell death mediators Bax and Bak: puzzles and conundrums. Cell Cycle. 2008; 7:39–44. [PubMed: 18196961]

Fletcher JI, Meusburger S, Hawkins CJ, Riglar DT, Lee EF, Fairlie WD, Huang DC, Adams JM. Apoptosis is triggered when prosurvival Bcl-2 proteins cannot restrain Bax. Proc Natl Acad Sci U S A. 2008; 105:18081–18087. [PubMed: 18981409]

Franklin JL, Johnson EM Jr. Elevated intracellular calcium blocks programmed neuronal death. Ann N Y Acad Sci. 1994; 747:195–204. [PubMed: 7847671]

Goncalves RP, Buzhynskyy N, Prima V, Sturgis JN, Scheuring S. Supramolecular assembly of VDAC in native mitochondrial outer membranes. J Mol Biol. 2007; 369:413–418. [PubMed: 17439818]

Grimm S, Brdiczka D. The permeability transition pore in cell death. Apoptosis. 2007; 12:841–855. [PubMed: 17453156]

Harris MH, Vander Heiden MG, Kron SJ, Thompson CB. Role of oxidative phosphorylation in Bax toxicity. Mol Cell Biol. 2000; 20:3590–3596. [PubMed: 10779348]

Hoogenboom BW, Suda K, Engel A, Fotiadis D. The supramolecular assemblies of voltage-dependent anion channels in the native membrane. J Mol Biol. 2007; 370:246–255. [PubMed: 17524423]

Hsu YT, Wolter KG, Youle RJ. Cytosol-to-membrane redistribution of Bax and Bcl-X(L) during apoptosis. Proc Natl Acad Sci U S A. 1997; 94:3668–3672. [PubMed: 9108035]

Hsu YT, Youle RJ. Nonionic detergents induce dimerization among members of the Bcl-2 family. J Biol Chem. 1997; 272:13829–13834. [PubMed: 9153240]

Hsu YT, Youle RJ. Bax in murine thymus is a soluble monomeric protein that displays differential detergent-induced conformations. J Biol Chem. 1998; 273:10777–10783. [PubMed: 9553144]

Kim BJ, Ryu SW, Song BJ. JNK-and p38 kinase-mediated phosphorylation of Bax leads to its activation and mitochondrial translocation and to apoptosis of human hepatoma HepG2 cells. J Biol Chem. 2006; 281:21256–21265. [PubMed: 16709574]

Leber B, Lin J, Andrews DW. Embedded together: the life and death consequences of interaction of the Bcl-2 family with membranes. Apoptosis. 2007; 12:897–911. [PubMed: 17453159]

Linseman DA, Butts BD, Precht TA, Phelps RA, Le SS, Laessig TA, Bouchard RJ, Florez-McClure ML, Heidenreich KA. Glycogen synthase kinase-3beta phosphorylates Bax and promotes its mitochondrial localization during neuronal apoptosis. J Neurosci. 2004; 24:9993–10002. [PubMed: 15525785]

Majewski N, Nogueira V, Bhaskar P, Coy PE, Skeen JE, Gottlob K, Chandel NS, Thompson CB, Robey RB, Hay N. Hexokinase-mitochondria interaction mediated by Akt is required to inhibit

apoptosis in the presence or absence of Bax and Bak. Mol Cell. 2004; 16:819–830. [PubMed: 15574336]

Miller TM, Moulder KL, Knudson CM, Creedon DJ, Deshmukh M, Korsmeyer SJ, Johnson EM Jr. Bax deletion further orders the cell death pathway in cerebellar granule cells and suggests a caspase-independent pathway to cell death. J Cell Biol. 1997; 139:205–217. [PubMed: 9314540]

Narita M, Shimizu S, Ito T, Chittenden T, Lutz RJ, Matsuda H, Tsujimoto Y. Bax interacts with the permeability transition pore to induce permeability transition and cytochrome c release in isolated mitochondria. Proc Natl Acad Sci U S A. 1998; 95:14681–14686. [PubMed: 9843949]

Pastorino JG, Shulga N, Hoek JB. Mitochondrial binding of hexokinase II inhibits Bax-induced cytochrome c release and apoptosis. J Biol Chem. 2002; 277:7610–7618. [PubMed: 11751859]

Polcic P, Forte M. Response of yeast to the regulated expression of proteins in the Bcl-2 family. Biochem J. 2003; 374:393–402. [PubMed: 12780347]

Ren D, Kim H, Tu HC, Westergard TD, Fisher JK, Rubens JA, Korsmeyer SJ, Hsieh JJ, Cheng EH. The VDAC2-BAK rheostat controls thymocyte survival. Sci Signal. 2009; 2:ra48. [PubMed: 19706873]

Robey RB, Hay N. Mitochondrial hexokinases, novel mediators of the antiapoptotic effects of growth factors and Akt. Oncogene. 2006; 25:4683–4696. [PubMed: 16892082]

Roucou X, Montessuit S, Antonsson B, Martinou JC. Bax oligomerization in mitochondrial membranes requires tBid (caspase-8-cleaved Bid) and a mitochondrial protein. Biochem J. 2002; 368:915–921. [PubMed: 12193163]

Schagger H, Cramer WA, Von JG. Analysis of molecular masses and oligomeric states of protein complexes by blue native electrophoresis and isolation of membrane protein complexes by two-dimensional native electrophoresis. Anal Biochem. 1994; 217:220–230. [PubMed: 8203750]

Schagger H, Von JG. Blue native electrophoresis for isolation of membrane protein complexes in enzymatically active form. Anal Biochem. 1991; 199:223–231. [PubMed: 1812789]

Shimizu S, Narita M, Tsujimoto Y. Bcl-2 family proteins regulate the release of apoptogenic cytochrome c by the mitochondrial channel VDAC. Nature. 1999; 399:483–487. [PubMed: 10365962]

Tsujimoto Y, Shimizu S. The voltage-dependent anion channel: an essential player in apoptosis. Biochimie. 2002; 84:187–193. [PubMed: 12022949]

Upton JP, Valentijn AJ, Zhang L, Gilmore AP. The N-terminal conformation of Bax regulates cell commitment to apoptosis. Cell Death Differ. 2007; 14:932–942. [PubMed: 17273174]

Valentijn AJ, Upton JP, Gilmore AP. Analysis of endogenous Bax complexes during apoptosis using blue native PAGE: implications for Bax activation and oligomerization. Biochem J. 2008; 412:347–357. [PubMed: 18307410]

Wolter KG, Hsu YT, Smith CL, Nechushtan A, Xi XG, Youle RJ. Movement of Bax from the cytosol to mitochondria during apoptosis. J Cell Biol. 1997; 139:1281–1292. [PubMed: 9382873]

Yethon JA, Epand RF, Leber B, Epand RM, Andrews DW. Interaction with a membrane surface triggers a reversible conformational change in Bax normally associated with induction of apoptosis. J Biol Chem. 2003; 278:48935–48941. [PubMed: 14522999]

Youle RJ, Strasser A. The BCL-2 protein family: opposing activities that mediate cell death. Nat Rev Mol Cell Biol. 2008; 9:47–59. [PubMed: 18097445]

Yuan S, Fu Y, Wang X, Shi H, Huang Y, Song X, Li L, Song N, Luo Y. Voltage-dependent anion channel 1 is involved in endostatin-induced endothelial cell apoptosis. FASEB J. 2008; 22:2809–2820. [PubMed: 18381814]
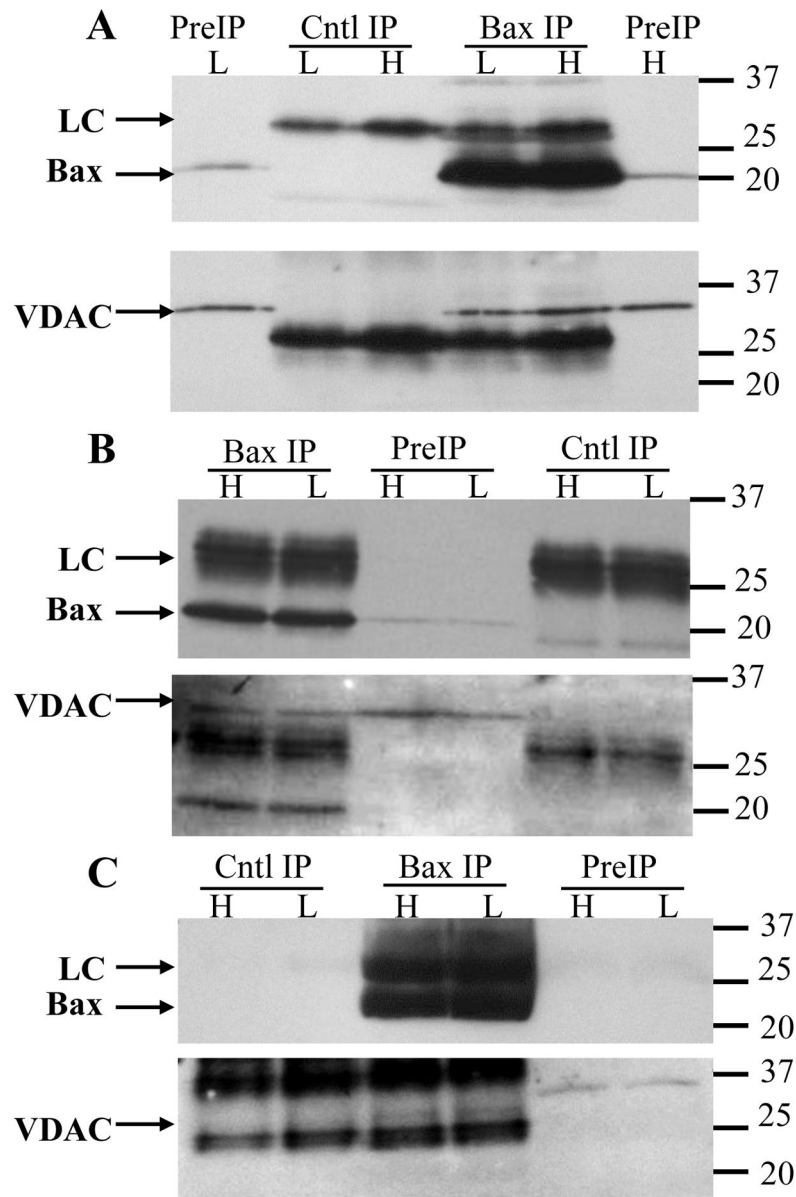
Figure 1. VDAC1 co-immunoprecipitates with Bax
Granule neurons were maintained in high or low K for 5h then solubilized with 1%
digitonin. The extracts were immunoprecipitated with the 1D1 antibody, or an irrelevant
mouse monoclonal (A, C) or goat polyclonal (B) antibody (as control), separated by SDS-
PAGE, blotted to PVDF membranes, then probed for Bax (top image of each pair), stripped,
and re-probed for VDAC1. Three independent experiments are shown in A–C to
demonstrate the variable recovery of VDAC1. (A) High VDAC1 recovery with 14 million
neurons solubilized with 700µl. Protein concentrations in the high K control and 1D1
extracts were 557 and 547 µg/ml, respectively, and in the low K control and 1D1 extracts
were 551 and 567 µg/ml, respectively. Prior to immunoprecipitation, the samples were
concentrated to final protein concentrations of 1331, 1459, 1460, and 1450 µg/ml,
respectively. (B) Moderate VDAC1 recovery with 6 million neurons solubilized with 525 µl.
Protein concentrations were not determined in this experiment. The extracts were not
concentrated prior to immunoprecipitation. (C) Weak VDAC1 recovery with 10.5 million

neurons solubilized with 525 μl. Protein concentrations in the high K control and 1D1 extracts were 769 and 717 μg/ml, respectively, and in the low K control and 1D1 extracts were 491 and 495 μg/ml, respectively. Prior to immunoprecipitation, the samples were concentrated to final protein concentrations of 1986, 1930, 1235, and 1319 μg/ml, respectively. Occasionally, as in image C, the secondary antibody did not bind the control antibody light chain as strongly as the 1D1 light chain (although this was not true for the heavy chain; not shown), which resulted in undetectable light chains with short exposure times. The absence of Bax in the preIP lanes is also due to the short exposure time. Longer exposures confirmed the presence of the light chains and preIP Bax (not shown). Both Bax and VDAC1 in the initial extracts occasionally migrated more slowly than in the immunoprecipitates, which was attributed to interference by excess loading of digitonin. Molecular weight markers are indicated to the right of the blots. H: high K; L: low K; PreIP: initial digitonin extract; Cntl IP: control immunoprecipitation; Bax IP: Bax 1D1 immunoprecipitation; LC: antibody light chain.
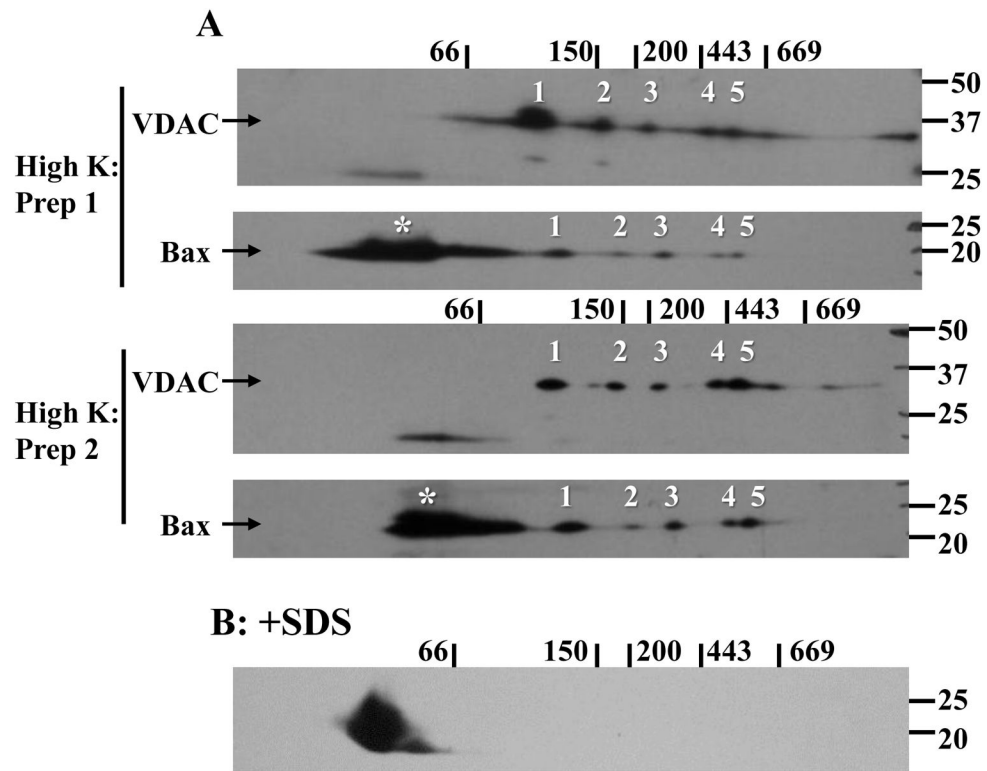
Figure 2. Bax and VDAC1 oligomers identified in healthy neurons by 2-dimensional gel electrophoresis

High K digitonin extracts were subjected to BN-SDS PAGE and blotted to PVDF membranes as detailed in the Methods section. The membranes were probed for Bax and VDAC1 with polyclonal N20 and N18 antibodies, respectively. (A) Representative images from two of five experiments are shown. Molecular mass markers for the first and second dimensions are indicated above and to the right, respectively, of the blots. Bax oligomers 1–5 (numbered) were routinely identified and closely resembled the pattern observed for the five indicated VDAC1 oligomers. The asterisks denote low molecular mass, presumably monomeric, Bax as the migration was similar to that seen when the extract was spiked with 1% SDS (B).
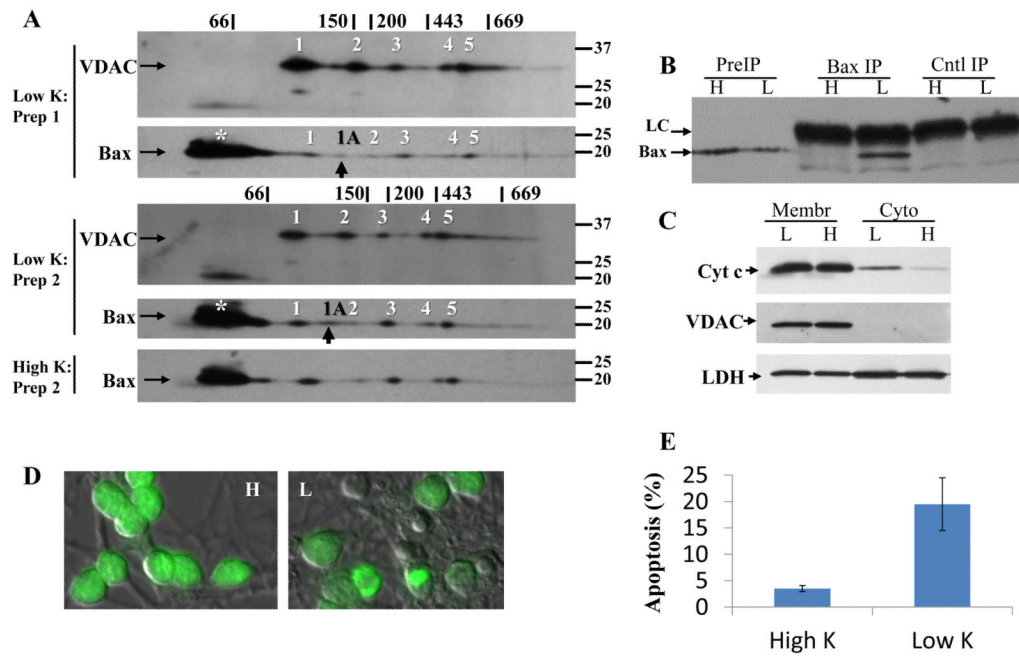
Figure 3. Bax and VDAC1 oligomers identified in apoptotic neurons by 2-dimensional gel electrophoresis
(A) Low K digitonin extracts were subjected to BN-SDS PAGE as described in Fig. 2. Representative images from two of five experiments are shown. The five oligomers equivalent to those identified in healthy neurons are indicated with numbers. An additional Bax oligomer not seen in healthy neurons, indicated with a black arrow and designated as 1A, was also identified. For comparison, the Bax oligomers from cells maintained in high K is shown. The asterisk identifies monomeric Bax (see Fig. 2). (B) The presence of oligomer 1A coincides with immunoprecipitation of the active 6A7 Bax conformation. Each extract was prepared from 4×10^6 neurons. H: high K; L: low K; PreIP: initial digitonin extract; Cntl IP: control immunoprecipitation; Bax IP: Bax 6A7 immunoprecipitation; LC: antibody light chain. (C) The presence of oligomer 1A coincides with cytochrome c release. Crude cytosolic extracts were prepared by plasma membrane permeabilization of 7×10^6 neurons with 20 μg/ml digitonin for 3min at 4°C, followed by solubilization of the remaining membrane (Membr) fraction with 1% SDS. The fractions (7 μg protein) were separated by SDS-PAGE and immunoblotted against cytochrome c (cyt c), VDAC1 (as a mitochondrial membrane marker), and lactate dehydrogenase (LDH, as a cytoplasmic marker). Cytoplasmic cytochrome c content was assessed by densitometry, and normalized to the level of cytoplasmic LDH. Images from one of two experiments are shown. (D) SYTO13-staining (green) of granule neurons after 5h in high (H) or low (L) K. Condensation and fragmentation of nuclear DNA as well as cell shrinkage (as indicated by differential interference contrast image superimposed with SYTO13 staining) is evident in low K. (E) Apoptosis was quantified after 5h in high or low K by counting at least 500 SYTO13-stained cells per treatment per experiment. Data are mean±S.E.M. of 4 experiments.
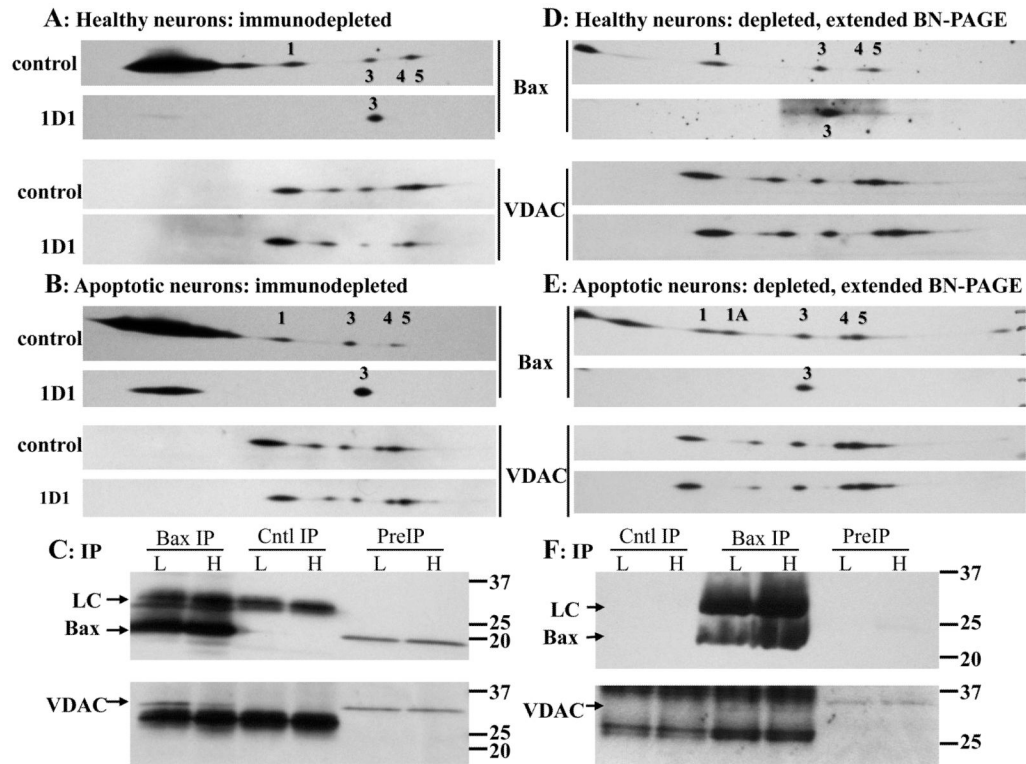
Figure 4. Analysis of Bax and VDAC1 oligomers following 1D1 Bax immunodepletion
(A, B) Ten million neurons maintained in high (A) or low (B) K for 5h were solubilized
with 525µl 1% digitonin. Protein concentrations in the high K control and 1D1 extracts were
438 and 521 µg/ml, respectively, and in the low K control and 1D1 extracts were 367 and
423 µg/ml, respectively. Prior to immunoprecipitation, the samples were concentrated to
final protein concentrations of 993, 1403, 982, and 944 µg/ml, respectively. The extracts
were immunodepleted of Bax overnight with the 1D1 antibody or an irrelevant mouse
monoclonal antibody as control (top image of each pair). Aliquots (25µg protein) were
subjected to BN-SDS PAGE, and immunoblotted for Bax and VDAC1 using the 1D1 and
N18 antibodies, respectively. Bax oligomer 3 resisted immunoprecipitation. Note that
oligomer 1A is not detectable in B. (C) Analysis of the immunoprecipitates from A and B
for Bax and VDAC1, demonstrating strong recovery of VDAC1. (D, E) Seven million
neurons maintained in high (D) or low (E) K were solubilized with 350 µl 1% digitonin.
Protein concentrations in the high K control and 1D1 extracts were 698 and 641 µg/ml,
respectively, and in the low K control and 1D1 extracts were 595 and 691 µg/ml,
respectively. Prior to immunoprecipitation, the samples were concentrated to final protein
concentrations of 1664, 1529, 1430, and 1612 µg/ml, respectively. The depleted samples
were processed as above except that 36 µg protein was loaded, and the BN PAGE was
performed for 240 min rather than 120 min to increase separation of the oligomers (with one
consequence being that most of the monomer had migrated off the bottom of the gel). No
change in VDAC1 oligomer intensities were observed (see Table 3). Representative images
from 2 of 4 independent experiments are shown. (F) Analysis of the immunoprecipitates
from D and E for Bax and VDAC, demonstrating weak recovery of VDAC1. As in Fig. 1,
the control antibody light chain and preIP Bax are not detectable with the short exposure
time. H: high K; L: low K; PreIP: initial digitonin extract; Cntl IP: control
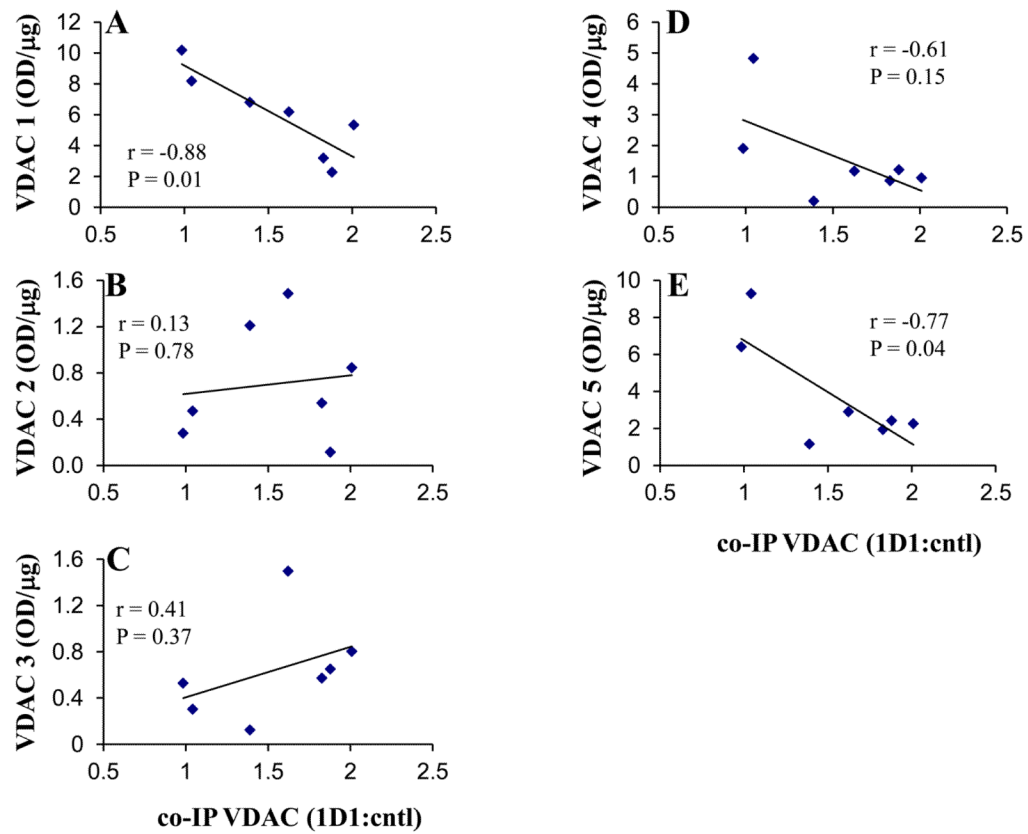immunoprecipitation; Bax IP: Bax 1D1 immunoprecipitation; LC: antibody light chain.

Figure 5. Correlation of VDAC1 oligomer levels in 1D1 depleted extracts to VDAC1 recovered in the immunoprecipitates

VDAC1 oligomers 1–5 (A–E, respectively) intensities (normalized per µg protein loaded) following Bax 1D1 immunodepletion were plotted against VDAC1 recovered in the immunoprecipitates (expressed relative to control lanes, and normalized to starting cell number). The high and low K data were combined for the analysis. Correlation coefficients (r) and P-values resulting from two-tailed correlation analyses are provided. The coefficients of determination (R^2) for oligomers 1–5 from the linear regressions were 0.77, 0.02, 0.16, 0.37, and 0.59, respectively.
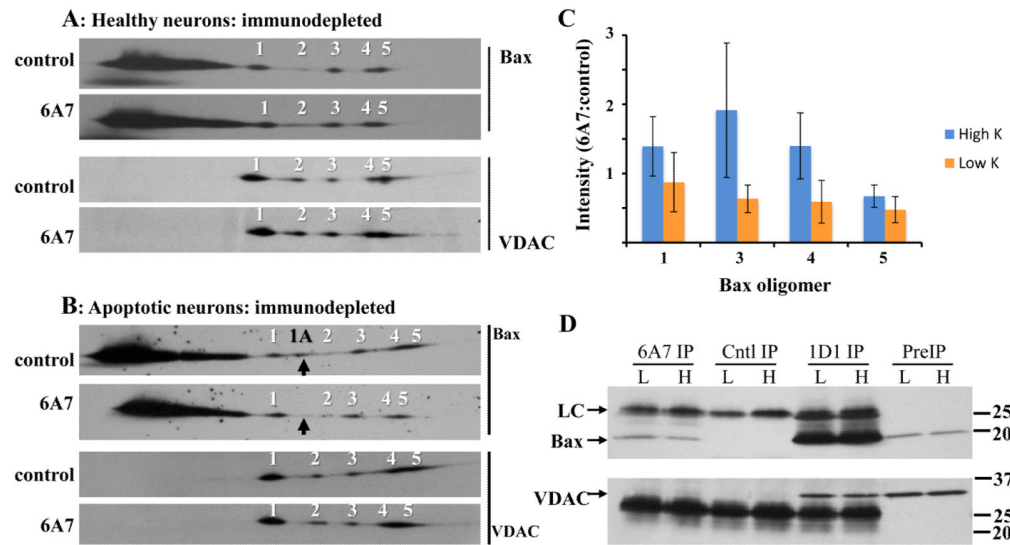
Figure 6. Analysis of Bax and VDAC1 oligomers following 6A7 Bax immunodepletion
Fourteen million neurons maintained in high (A) or low (B) K for 5h were solubilized with 700µl 1% digitonin. Protein concentrations in the high K control and 1D1 extracts were 540 and 502 µg/ml, respectively, and in the low K control and 1D1 extracts were 400 and 502 µg/ml, respectively. Prior to immunoprecipitation, the samples were concentrated to final protein concentrations of 1253, 1211, 964, and 1203 µg/ml, respectively. The extracts were immunodepleted of active Bax overnight with the 6A7 antibody, or with an irrelevant mouse monoclonal antibody as control (top image of each pair). Aliquots (25µg protein) were subjected to BN SDS-PAGE, and immunoblotted for Bax and VDAC1 using the 1D1 and N18 antibodies, respectively. Images are from one of three independent experiments. The 6A7 antibody depleted the low K extracts of virtually all 1A oligomer, as indicated with the black arrows. (C) Quantification of Bax oligomers 1, 3, 4, and 5 in high and low K 6A7 depleted extracts; oligomer 2 was excluded due to inconsistent detection. Oligomer levels were normalized to the corresponding controls. Statistical analysis by 2-way ANOVA (treatment [high, low K] and oligomer as main effects) yielded a significant effect of treatment (P=0.049) but not of oligomer (P=0.489), with no significant treatment-oligomer interaction (P=0.694). Data are mean ± SEM of three experiments. (D) VDAC1 was undetectable in both high and low K Bax 6A7 immunoprecipitates, but was readily identified in parallel Bax 1D1 samples. H: high K; L: low K; PreIP: initial digitonin extract; Cntl IP: control immunoprecipitation; 6A7 IP: Bax 6A7 immunoprecipitation; 1D1 IP: Bax 1D1 immunoprecipitation; LC: antibody light chain.
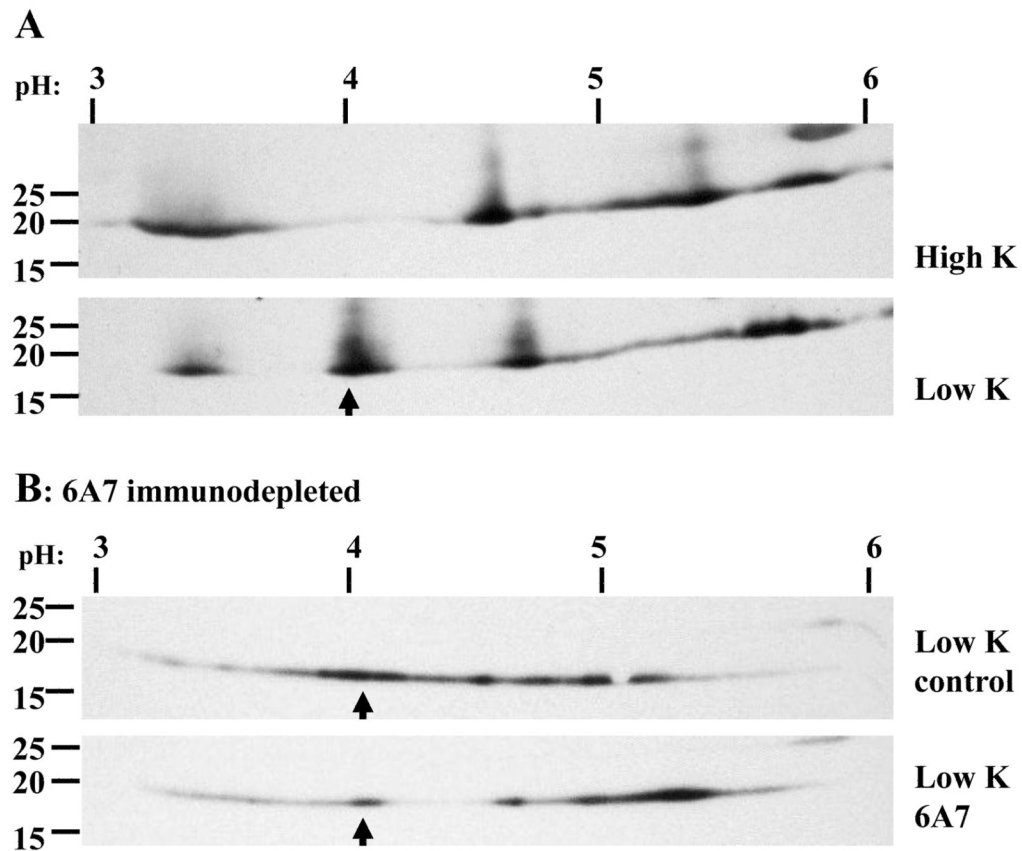
Figure 7. Bax post-translational modification in high and low K assessed by IEF-SDS PAGE
(A) Seven-million CGNs exposed 5h to high or low K were solubilized with 350 μl 1% digitonin and immunoprecipitated overnight with the 1D1 antibody without prior concentration. The initial protein concentrations were not determined. Immunoprecipitates were eluted in IEF sample buffer containing DTT, focused on pH 3–6 IPG strips, then subjected to second dimension SDS-PAGE and western blotting. The top and bottom images are the high and low K extracts, respectively. The pH gradient and molecular mass markers are indicated above and to the left of the images, respectively. Low K resulted in a modification that shifted the isoelectric point to approximately 4.0 (indicated with an arrow). (B) Digitonin extracts were immunodepleted of 6A7 Bax overnight at 4°C. Residual Bax was immunoprecipitated for 2h at room temperature (≈23°C) and processed as in (A). Immunodepletion with the 6A7 antibody reduced the abundance of the apoptotic-specific post-translational modification, indicated by arrows.
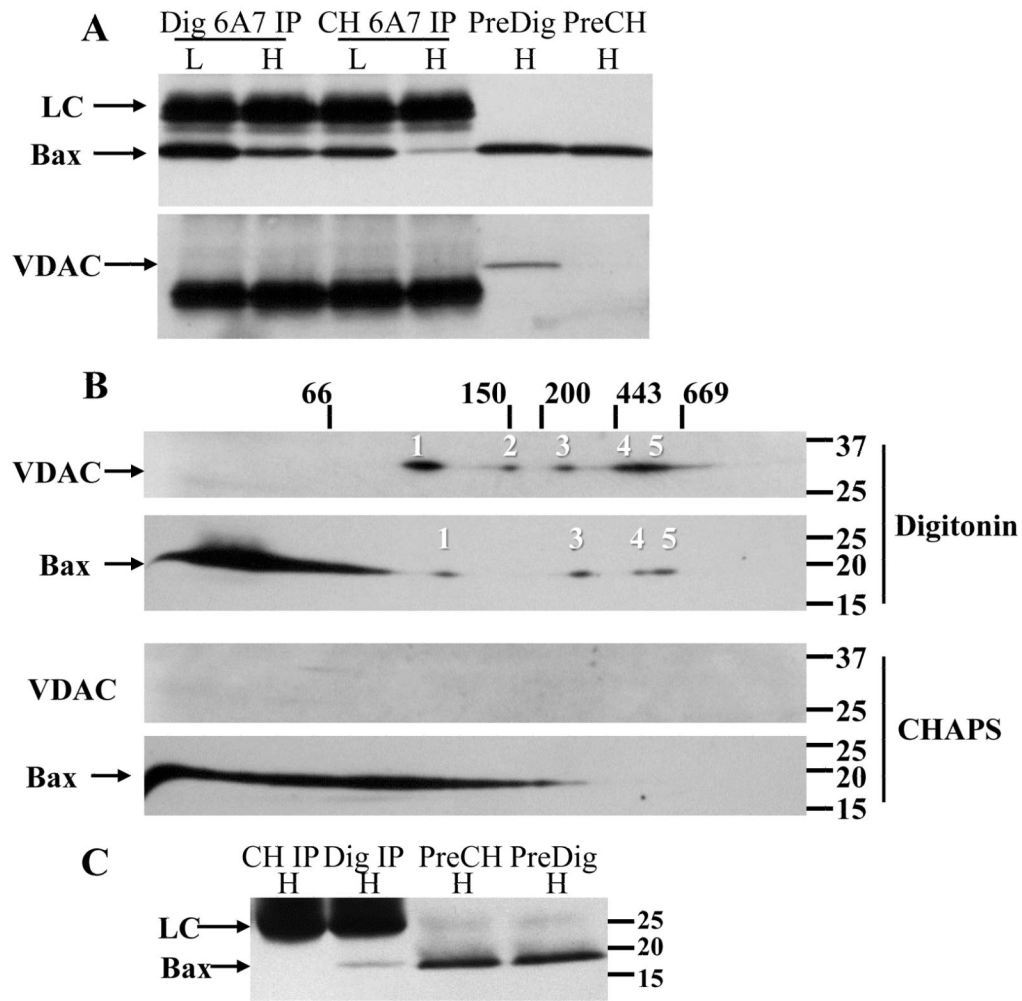
Figure 8. Oligomer pattern and 6A7 Bax recovery fromCHAPS and digitonin extracted neurons
Ten million neurons were maintained in high or low K for 5h, solubilized with 700 μl 1%
digitonin or CHAPS, then immunodepleted of active Bax overnight with the 6A7 antibody.
Protein concentrations in the high and low K digitonin extracts were 340 and 390 μg/ml,
respectively, and in the high and low K CHAPS extracts were 393 and 442 μg/ml,
respectively. Prior to immunoprecipitation, the samples were concentrated to final protein
concentrations of 783, 1060, 867, and 922 μg/ml, respectively. (A) Western blot of Bax (top
image) and VDAC1 (bottom image) recovered in the 6A7 immunoprecipitates, detected
with the 1D1 (for Bax) or N18 (for VDAC1) antibodies. Note that VDAC1 was undetectable
in the initial CHAPS extract. (B) High K digitonin (top two images) and CHAPS (bottom
two images) extracts (25μg protein) depleted of 6A7 Bax were further analyzed by 2D BN
SDS-PAGE. The typical Bax and VDAC oligomeric pattern with digitonin was not observed
with CHAPS. (C) Cytosolic extracts from 14×10^6 healthy neurons were prepared with 700
μl detergent-free extraction buffer. The extract (initial protein concentration not determined)
was divided equally and supplemented with either 1% digitonin or CHAPS, then
immunoprecipitated with the 6A7 antibody and Western blotted against Bax with the 1D1
antibody. H: high K; L: low K; Dig IP: 6A7 immunoprecipitation in 1% digitonin; CH IP:
6A7 immunoprecipitation in 1% CHAPS; PreDig: initial extract prepared with digitonin;
PreCH: initial extract prepared with CHAPS; LC: antibody light chain.

Table 1

Bax and VDAC1 densitometry analysis of 1D1 immunoprecipitates.

	Bax	VDAC
High K	13.4±2.2	1.6±0.3
Low K	13.6±5.2	1.7±0.4

Bax 1D1 immunoprecipitations were separated by SDS-PAGE, western blotted, then probed for Bax and VDAC. The films were digitized and the band intensities quantified using Image J software. The intensities were normalized to the adjacent regions within the control lanes. The data are mean±SEM of five experiments where VDAC1 was positively identified.

Table 2

Bax and VDAC1 oligomer molecular masses determined by BN-SDS PAGE.

Oligomer	Healthy		Apoptotic	
	Bax (kDa)	VDAC (kDa)	Bax (kDa)	VDAC (kDa)
1	125±8	106±4	131±17	113±10
2	190±10	174±6	212±31	186±14
3	272±9	243±9	307±34	270±19
4	415±18	371±19	466±51	418±29
5	489±22	446±23	562±63	505±35
1A	-	-	168±19	-

Digitonin solubilized extracts prepared from CGNs exposed 5h to high (healthy) or low (apoptotic) K for 5h were subjected to BN-SDS PAGE and western blotted for Bax and VDAC1 as described in Figs. 2 and 3. Oligomers 1 through 5 are those identified by numbers in Figs 2 and 3; oligomer 1A is that indicated by arrows in Fig. 3. Gel filtration standards (thyroglobulin 669, apoferritin 443, β-amylase 200, alcohol dehydrogenase 150, and albumin 66 kDa) run in the first dimension were used to determine the molecular masses. Statistical analysis by 2-way ANOVA indicated no significant effects of protein (Bax/VDAC) ($p = 0.10$, 0.23, 0.13, 0.17, and 0.22 for oligomers 1, 2, 3, 4, and 5, respectively), treatment (low/high K) ($p = 0.55$, 0.49, 0.15, 0.14, and 0.11 for oligomers 1, 2, 3, 4, and 5, respectively), or protein-treatment interaction ($p = 0.99$, 0.76, 0.84, 0.94, and 0.87, respectively) on the oligomers. This indicates the molecular masses of the Bax oligomers do not significantly differ from the corresponding VDAC1 oligomers, and low K treatment does not significantly affect oligomer mass. Data are mean±SEM of five independent preparations.

Table 3

Densitometry of VDAC1 oligomers identified by BN-SDS PAGE following Bax 1D1 immunodepletion.

	VDAC: Healthy neurons		VDAC: Apoptotic neurons	
Oligomer	control deplete	1D1 deplete	control deplete	1D1 deplete
1	5.37±1.29	7.73±1.08	5.39±2.14	4.55±1.83
2	0.66±0.08	0.95±0.26	0.61±0.32	0.37±0.13
3	0.59±0.10	0.74±0.29	0.56±0.23	0.51±0.10
4	0.94±0.17	1.06±0.35	0.99±0.16	2.30±1.27
5	1.84±0.18	3.18±1.14	2.82±0.84	4.54±2.37

Digitonin solubilized extracts prepared from CGNs exposed 5h to high (healthy) or low (apoptotic) K were incubated overnight at 4°C with a Bax 1D1 or control mouse monoclonal antibody. The extracts were cleared of antibody complexes using Protein G Dynabeads then subjected to BN-SDS PAGE and western blotting as indicated in Fig. 4. VDAC1 oligomer intensities after immunodepletion were calculated using Image J software as the sum of pixel intensities (in optical density units) within the elliptical area of each spot. Statistical analysis by 2-way ANOVA indicated no significant effects of antibody [control, 1D1] (p= 0.77, 0.89, 0.83, 0.24, and 0.25 for oligomers 1, 2, 3, 4, and 5, respectively), treatment [high, low K] (p= 0.40, 0.18, 0.56, 0.29, and 0.37 for oligomers 1, 2, 3, 4, and 5, respectively), or antibody-treatment interaction (p= 0.41, 0.25, 0.64, 0.33, and 0.88 for oligomers 1, 2, 3, 4, and 5, respectively) on the abundance of the VDAC1 oligomers. Bax oligomer depletion therefore does not significantly affect the amount of each corresponding VDAC1 oligomer. Data are mean ± SEM of three (low K) or four (high K) experiments.